Layered Structure and Vs30 at Colocated Pressure and Seismic Stations in the Transportable Array

Jiong Wang and Toshiro Tanimoto

Department of Earth Science, UCSB

Summary

- We propose a single-station inversion approach to estimate shallow layered elastic structure using ratios between pressure and seismic signals at low frequencies.
- At low frequencies (0.01 – 0.05 Hz), the solid Earth responds elastically to large atmospheric pressure variations (e.g. Sorrells 1971; Sorrells et al., 1971).
- We present our inversion procedure and Vs30 at 775 Transportable Array (TA) stations.
- We have estimated Vs30 at 9 co-located Piñon Flat Observatory (PFO) stations. Our results agree well with on-site measured Vs30 results.

Data and Halfspace Equations

Fig 1 shows the pressure-dependent seismic signals. Red points are power spectral densities (PSD) for the whole year of 2012 and green points are coherent time segments. In both horizontal and vertical components, pressure variations at 0.02 Hz correlate well with seismic signals.

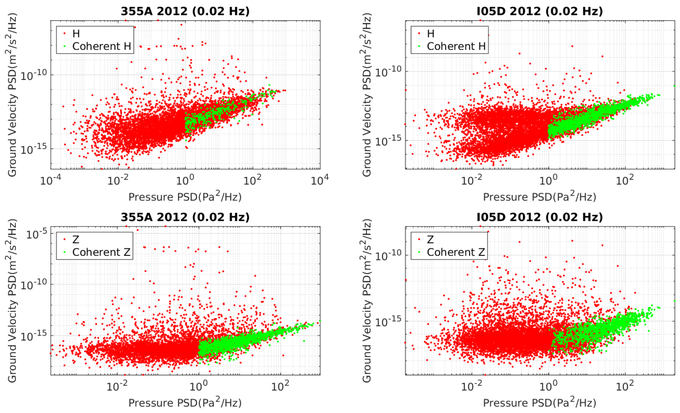

Figure 1. Comparison of ground velocity and pressure PSDs at two stations, 355A and I05D, at 0.02 Hz for the whole year of 2012. Each point is a one-hour PSD. Red points are all horizontal/vertical components PSDs; green points are PSDs with coherence higher than 0.7. 355A is a TA station located at Pearson, GA. I05D is a TA station located at Terrebonne, OR.

$$\frac{S_Z}{S_P} = \frac{c^2}{4\mu^2}\left(\frac{\lambda+2\mu}{\lambda+\mu}\right)^2 \quad (1)$$

$$\frac{S_H}{S_P} = \frac{g^2}{4\mu^2\omega^2}\left(\frac{\lambda+2\mu}{\lambda+\mu}\right)^2 \quad (2)$$

S_Z and S_H are PSDs of vertical and horizontal seismic components. S_P is PSDs of pressure. Detailed derivation can be found in Tanimoto and Wang (2018).

$$\overline{\mu} = \frac{g}{2\omega}\sqrt{\frac{S_P}{S_H}} \quad (3)$$

$$\overline{\mu} = \mu\frac{\lambda+\mu}{\lambda+2\mu} \quad (4)$$

$$coh(f) = \frac{|E[X^*(f)Y(f)]|}{\sqrt{E[|X(f)|^2]}\sqrt{E[|Y(f)|^2]}} \quad (5)$$

By rewriting equations 1 and 2, we obtain $\overline{\mu}$ by analyzing horizontal component only (equation 3). $\overline{\mu}$ from equation 4 is computed for this study. $\overline{\mu}$ is 2/3 of μ for the Poisson solid and 70 – 80 percent of μ for most crustal rocks. More rigorous empirical relations could be obtained (Brocher, 2005; Boore, 2016). We compute coherence between seismic and pressure data using equation 5.

Numerical Sensitivity Kernels

We compute sensitivity kernels of rigidity following the scheme proposed in Tanimoto and Wang (2019) using numerical differentiations. Kernels are mainly controlled by frequencies and pressure-wave speed c which can be calculated from equations 1 and 2 in the section above.

Fig 2 shows that our approach are estimating elastic rigidity for the top 50 or 100 meters at frequencies range from 0.01 to 0.05 Hz.

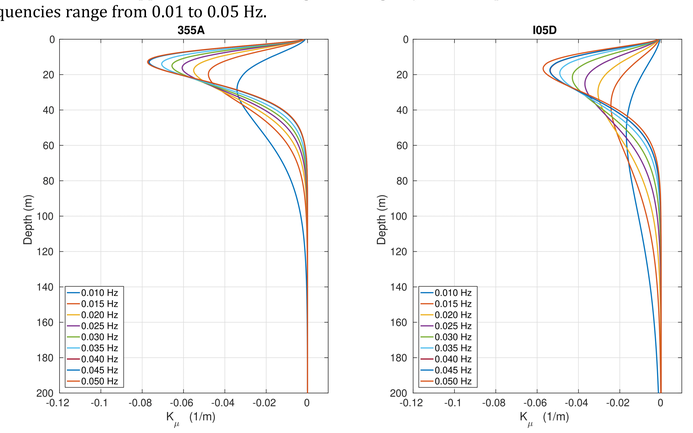

Figure 2. Depth sensitivity kernels of rigidity at two stations, 355A and I05D, at frequencies from 0.01 to 0.05 Hz, with an increment of 0.005 Hz.

Inversion Procedure and Results

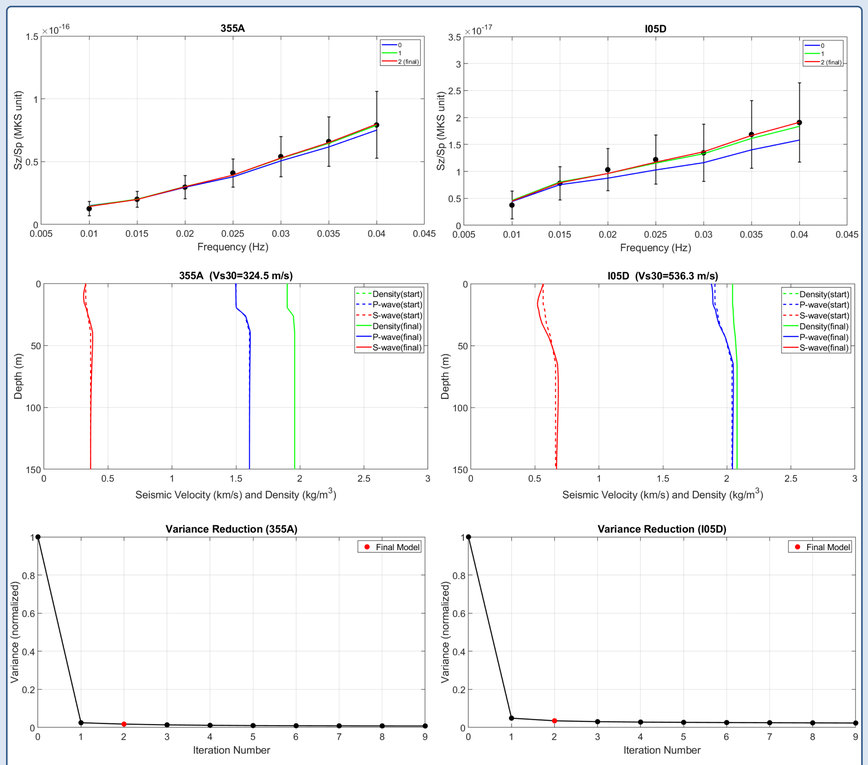

Figure 3. Inversion procedure for two TA stations, 355A and I05D. Top panels show how we fit the model to the observed data at surface stations. Middle panels show starting models and final models for both stations. Bottom panels demonstrate how to pick the final model by quantifying the improvement of misfit between each iterations.

Here are some summarized steps of the inversion approach. See detailed description in Tanimoto and Wang (2019).

1. We construct starting models for each station by using $\overline{\mu}$ obtained from halfspace estimations at different frequencies (between 0.01 Hz to up to 0.05 Hz) . Halfspace results at different frequencies provide Vp, Vs and density at different depths (see Figure 2).

2. The inversion process aims to fit the observable η(f)=Sz/Sp, as we can see in the top panels of Figure 3. We solve for layered medium of varying bulk modulus and rigidity, with a standard damped least squares approach.

3. In each iteration, we obtain a new layered structure. Typically, the inversion converges to the observables η(f) quickly after 1 or 2 iterations. In practice, we run 9 iterations and pick out the "final model" based on how much the misfit is improved. We quantify the misfit improvement by comparing the variance reduction between iterations, as we can see in the bottom panels of Figure 3.

4. After the "final model" is picked out, we can estimate Vs30 at each station with the layered structure, as we can see in the middle panels of Figure 3.

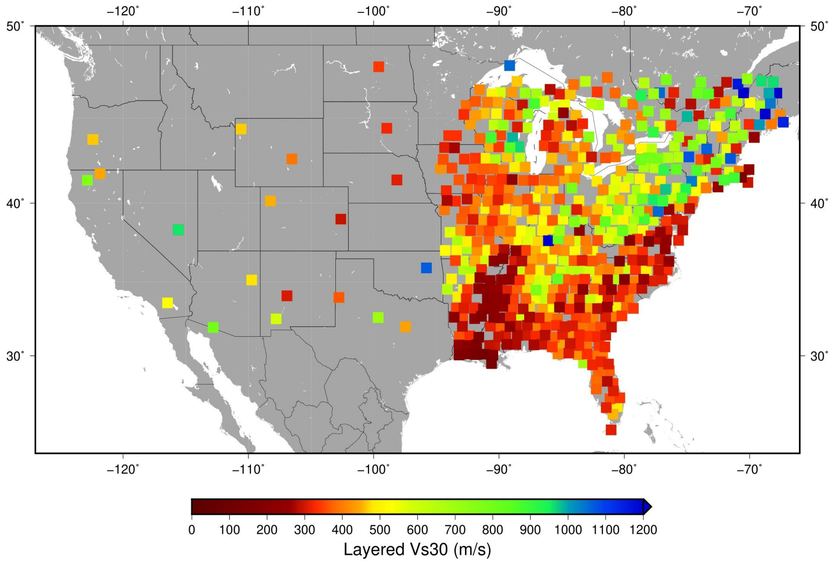

Figure 4. Map view of estimated Vs30 values at contiguous US TA stations. The color bar saturates at 1200 m/s.

Figure 4 presents a map view of estimated Vs30 values at many TA stations. Softer shallow structures are shown in red or yellow colors, and more rigid shallow structures are shown in green or blue colors.

Two noticeable features in the map are the Appalachian mountains region and the Mississippian Alluvium Plain. TA stations in the Appalachian mountains region typically have faster Vs30 and TA stations in the Mississippian Alluvium Plain typically have very slow Vs30. These two features are consistent with local geology.

Comparison with Measured Vs30

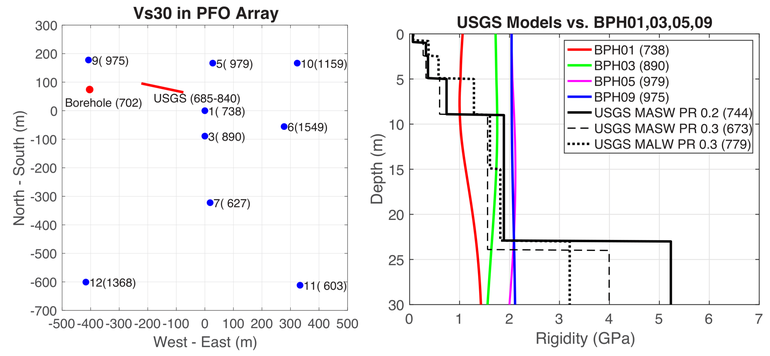

Figure 5: Comparison between our estimated Vs30 at 9 co-located PFO stations and on-site measured Vs30 values. Left panel presents our estimates of Vs30 at 9 PFO stations (blue circles). The number outside of the bracket is the station name and the number within the bracket is estimated Vs30 in m/s. Red circle is a borehole station described in Fletcher et al (1990) and Vs30 value is calculated from their S-wave speed model. Red lines show the geophone array in the USGS study (Yong et al. 2013). Their results contain several Vs30 estimates range from 685 m/s to 840 m/s, which come from various methods. Right panels show several elastic structure profiles from the USGS study, and estimated structure at 4 nearby PFO stations. Velocity profiles are converted into rigidity for comparisons.

We analyzed 9 stations within the Piñon Flat Observatory (PFO), network code PY. These 9 stations are broadband seismic stations, equipped with co-located barometers. More detailed data analysis can be found in Tanimoto and Wang (2020).

We estimated Vs30 at 9 different PFO stations. There is one on-site borehole with S-wave speed model from Fletcher et al. (1990) at the red circle in left panel of Figure 5. USGS (Yong et al. 2013) also have a study with Vs30 measured by geophone array along the red line in the left panel of Figure 5.

Estimates of Vs30 from USGS range from 685 m/s to 840 m/s. This range of Vs30 agrees well with our estimates at nearby PFO stations. For example, the closest station, BPH01, have an estimated Vs30 of 738 m/s.

In the left panel of Figure 5, we can see that Vs30 have quite large spatial variations even within a couple hundred meters.

In the right panel of Figure 6, we compare layered structures from our method and the USGS study. Although rigidity values agree within similar ranges, our profiles are much smoother than velocity profiles from higher-frequency geophone array studies such as MASW. However, because Vs30 is an averaged quantity for the top 30 meters, our estimates are reasonable and close to measured results.

Discussion

- In this study, we estimate Vs30 values at 775 TA stations by implementing the inversion approach we developed in Tanimoto and Wang (2019). Our results provide valuable structure information for seismic hazard studies.
- Our method is supported by comparing with on-site measured Vs30 within the Piñon Flat Observatory (PFO). Our estimates of Vs30 at nearby co-located stations agree well with the USGS study (Yong et al. 2013).
- Although layered structures obtained from our method are much smoother compared to higher-frequency active-source studies, our estimates of Vs30 are reasonable because Vs30 itself is an averaged quantity for the top 30 meters.

Acknowledgement

This project has been supported by SCEC (#19039, #20072) and USGS (G20AP00024).

We thank Frank Vernon and Joe Fletcher for providing detailed information on PFO stations. All data were acquired from IRIS (http://ds.iris.edu/mda) using ObsPY (Beyreuther et al,. 2010). We appreciate IRIS and code developers of ObsPy for their service. Figure 4 is made by GMT (Wessel et al,. 2013).

Reference

Beyreuther, M., R. Barsch, L. Krischer, T. Megies, Y. Behr, and J. Wassermann (2010), Obspy: A python toolbox for seismology, *Seismological Research Letters*, 81, 530–533, doi:10.1785/gssrl.81.3.530

Boore, D. M. (2016), Determining generic velocity and density models for crustal amplification calculations, with an update of the Boore and Joyner (1997) generic site amplification for, *Bulletin of the Seismological Society of America*, 106 (1), 313, doi:10.1785/0120150229.

Brocher, T. M. (2005), Empirical relations between elastic wave speeds and density in the earth's crust, *Bulletin of the Seismological Society of America*, 95 (6), 2081, doi:10.1785/0120050077.

Wessel, P., W. H. F. Smith., R. Scharroo, J. Luis, and F. Wobbe (2013), Generic mapping tools: Improved version released, Eos, *Transactions American Geophysical Union*, 94 (45), 409–410, doi:10.1002/2013EO450001.

Sorrells, G. G. (1971), A Preliminary Investigation into the Relationship between Long-Period Seismic Noise and Local Fluctuations in the Atmospheric Pressure Field, *Geophysical Journal of the Royal Astronomical Society*, 26 (1-4), 71–82, doi:10.1111/j.1365-246X.1971.tb03383.x.

Sorrells, G. G., J. A. McDonald, Z. A. Der, and E. Herrin (1971), Earth Motion Caused by Local Atmospheric Pressure Changes, *Geophysical Journal of the Royal Astronomical Society*, 26 (1-4), 83–98, doi:10.1111/j.1365-246X.1971.tb03384.x.

Tanimoto, T., and J. Wang (2018), Low-frequency seismic noise characteristics from the analysis of co-located seismic and pressure data, *Journal of Geophysical Research: Solid Earth*, 123, 5853-5885, doi:10.1029/2018JB015519.

Tanimoto, T., and J. Wang (2019), Theory for Deriving Shallow Elasticity Structure From Colocated Seismic and Pressure Data, *Journal of Geophysical Research: Solid Earth*, 124, 5811– 5835., doi:10.1029/2018JB017132.

Tanimoto, T., and J. Wang (2020), Shallow elasticity structure from colocated pressure and seismic stations in the Piñon Flat Observatory and estimation of Vs30, *Geophysical Journal International*, 222(1), 678–696, doi:10.1093/gji/ggaa195

Yong, A., Martin, A., Stokoe, K., and Diehl, J (2013), ARRA-funded VS30 measurements using multi-technique approach at strong-motion stations in California and central-eastern United States: U.S. Geological Survey Open-File Report 2013–1102, 60 p. and data files, http://pubs.usgs.gov/of/2013/1102/.